

D 1.2 Fuel Type Map at the national scale

D 1.3 Fuel model map parameterized for Rothermel-based fire behaviour applications

Work Package: WP1 – FUEL BOX

Work Package leader: UNITO

Deliverable leader: UNITO



NATIONAL RECOVERY AND RESILIENCE PLAN (NRRP) – MISSION 4

COMPONENT 2 – INVESTMENT 1.1: “Fund for the National Research Program and for
Projects of National Interest (PRIN)”

Project Acronym: FIRE-BOX

Project title: Essential tools for wildland fire risk management in Italy

Project code: P2022MXRK9

Duration of the project: 24 months



CITATION:

Ascoli D., Passamani C., Moris J.V., Spadoni G., Gamba R., Rainsford F. (2026). D1.3 Fuel model map parameterized for Rothermel-based fire behaviour applications. PRIN PNRR Project FIRE-BOX (P2022MXRK9). National Recovery and Resilience Plan (NRRP) – Mission 4, Component 2 Investment 1.1 – Fund for the National Research Program and for Projects of National Interest (NRP)”, Project FIRE-BOX – Essential tools for wildland fire risk management in Italy.

DISCLAIMER

Funded by the European Union and the Ministry of the University and Research. Views and opinions expressed are however those of the author(s) only and do not necessarily reflect those of the European Union. Neither the European Union nor the granting authority can be held responsible for them.



Executive summary

This deliverable synthesises the main outcomes of Deliverables D1.2 and D1.3 developed within WP1 of the FIRE-BOX project. Together, these outputs provide a harmonised national framework for mapping vegetation flammability and supporting wildfire behaviour modelling across Italy. In particular, D1.2 produces the national Fuel Type Map, while D1.3 develops the national Fuel Model Map for Rothermel-based fire behaviour applications. This deliverable combines D1.2 and D1.3, as they share a substantial part of the algorithm to generate both the Fuel Type and the Fuel model maps.

The Fuel Type Map is linked to Deliverable D1.1, from which it adopts the fuel type classification and the associated quantitative fuel database. D1.1 therefore provides the conceptual and empirical reference framework underlying the classification of mapped fuel types, ensuring consistency with the national system of fuel description developed within the project.

The overall methodology and the developed algorithm integrates nationally available spatial data on forest types, land cover, and vegetation structure with historical wildfire perimeters to derive a fire selectivity index as a proxy for relative flammability. This reproducible approach makes it possible to rank vegetation classes along a flammability gradient and to translate that gradient into both fuel types and operational fuel models.

The resulting products are complementary: the Fuel Type Map supports communication, planning, and hazard stratification, while the Fuel Model Map is intended for direct use in fire spread simulators such as FlamMap and other tools based on the Rothermel framework. Together, they represent a nationally consistent and updateable basis for wildfire risk assessment, fire management planning, and decision-support applications in Italy.

Keywords

Fuel models; Rothermel; fire behaviour; Italy; fuel mapping; fire selectivity; CFI2020; NDVI; reproducible workflow



Table of contents

1. Introduction.....	5
1.1. Physiognomic approaches to calibrate fuel model maps	5
1.2. FIREBOX approach.....	6
2. Data architecture and national harmonisation framework.....	9
2.1. Terminology and Classification Framework	9
2.2. Italian Forest Map (CFI2020).....	10
2.3. Corine Land Cover 2018	12
3. Algorithm workflow	17
3.1. Regional Workflow: Sub-Class Segmentation and Raster Construction	17
3.2. Fire Selectivity Computation and Statistical Aggregation	21
4. National Fuel Model Association and Clustering.....	25
4.1. Fuel group classification.....	26
4.2. Selection of candidate fuel models	26
4.3. Clustering procedure.....	28
4.4. Production of the fuel model map	29
4.5. Implications	29
5. Validation and Performance Assessment.....	31
5.1. Coherence in the selectivity index gradient of macro- and sub-classes	31
5.2. Regional-scale simulated potential fireline intensity.....	34
5.3. Assessment of potential fireline intensity relative to historical fire perimeters	34
6. Fuel model map methodological assumptions and limitations.....	40
7. Fuel Type map	42
7.1. National flammability thresholds	43
7.2. Fuel type coding system	45
8. Operational implications of the Fuel Model and Fuel Type maps.....	46

ANNEX

Annex A - Fuel model map

Annex B – Fuel Type map



1. Introduction

Deliverable D1.3 provides the national fuel model map produced within WP1-FUELBOX, i.e. Milestone 3, the detailed workflow used to generate it, as implemented through an algorithm in R, the validation tests, and final considerations about limitations of the algorithm implemented, and its potentials. The objective of WP1 was to invent an open access algorithm that translates spatial information (forest typologies, land cover, and remotely sensed proxies of vegetation structure) available at the national-scale into a fuel model layer that can drive operational and research fire behaviour simulations using the CNR fire simulator (see Deliverable 3.2), and other decision support systems based on the Rothermel (1972) surface spread model, e.g., FlamMap model (Finney 2004), Rothermel package in R (Vacchiano & Ascoli 2015). The innovative approach we tested is grounded on several assumptions, here after briefly introduced, and aims at improving current limitations in the state of art of approaches to calibrate Rothermel (1972) fuel models maps over large scales.

1.1. Physiognomic approaches to calibrate fuel model maps

Wildland fuels vary along multiple dimensions such as physiological activity and moisture content (live vs. dead), particle size distribution, spatial arrangement, and seasonal dynamics. In fire science, a fuelbed describes qualitatively and quantitatively these characteristics, while a fuel model is a standardized, simplified description of the fuelbed designed to parameterize the input of a fire spread model (Keane 2015). Standard operational fuel model catalogues to be used as input of the Rothermel (1972) model, e.g., the original 10 “fire behaviour fuel models” (Rothermel 1972), the improved 13 fuel models by Anderson (1982) set, and later expansions such as the 40 fuel models of Scott & Burgan (2005), have been developed to display a gradient of fire behaviour within a range of rate of spread (ROS) and fireline intensity (FI) as observed in nature. The practicality of fuel models is that they allow consistent, repeatable calculations of fire behaviour metrics such as rate of spread (ROS) or fireline intensity (FI). The challenge is that fuel models inevitably compress real-world fire behaviour variability into a finite set of stylized and “abstract” fuel models (e.g., Anderson 1982) whose parameterization does not correspond to average fuel conditions observed in nature in a given fuel complex (Rothermel 1972).



Historically, fuel models' assignment to a set of fuelbeds and their mapping focused on the physiognomic characteristics of the dominant vegetation in each land-use class, and on the matching between average fuel characteristics of the fuelbed and fuel model parameters. This approach consists in defining for each land-use class the main fuel component carrying the fire (e.g., grass, hardwood or conifer litter, deadwood), estimating the amount of dry fuel in different classes (1h, 10h, 100h dead fuels, and live grasses and shrubs), and then associating one of the standard fuel models based on the matching of physiognomy and loadings (e.g., Wu et al. 2011, Parresol et al. 2012). The underlying assumption of this approach is that, if a fuel bed is characterised, for example, by a low-porosity hardwood litter layer in the absence of understory vegetation, the most “representative” fuel model under a physiognomic approach would be TL2 (182) – Low Load Broadleaf Litter (Scott & Burgan 2005), where the primary carrier of fire is broadleaf (hardwood) litter characterised by a low load and compact structure. However, this approach can create discrepancies between simulated and observed fire behaviour because the standard fuel model that is most similar from a physiognomic perspective does not necessarily provide the best simulation in terms of minimizing error between simulated and observed rate of spread (Ascoli et al. 2022). The original approach proposed by Rothermel (1972) was to associate fuel models to vegetation classes based on the expected fire behaviour in a fuel bed under certain fuel moisture, topographic and weather conditions. However, this approach has been rarely implemented at the stand scale (Cruz & Fernandes 2008, Ascoli et al. 2015) and has no application at the large scale for calibrating fuel model maps.

1.2. FIREBOX approach

Within the FIREBOX project, we proposed a new approach to calibrate a fuel model map for the whole Italy. The method consists of identifying fuel groups (i.e., grasses, shrubs, broadleaves forests fuelbeds, conifers forests fuelbeds, agriculture burnable), and rank land-use classes within a given fuel group along an increasing flammability gradient estimated quantitatively. In parallel, a set of fuel models is assigned to the same fuel group and ranked according to simulated rate of spread (ROS). Each fuel model is then matched to a land-use class within the macro fuel group based on the corresponding ranking (Figure 1).

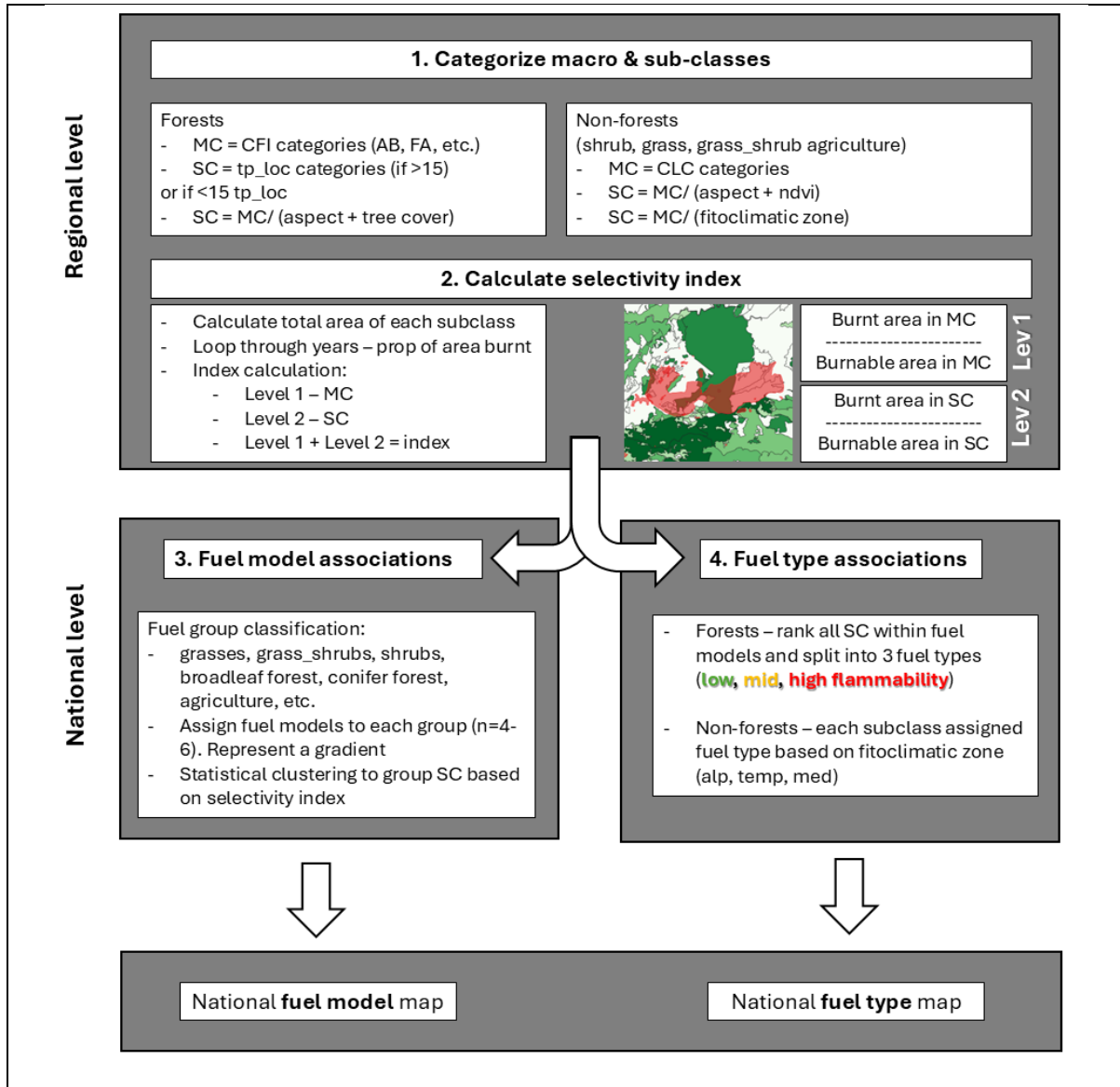


Figure 1 – FIREBOX workflow to generate the national fuel model map.

The set of fuel models associated with each fuel group follows two criteria: (i) it is selected from the standard fuel models calibrated for that fuel group by Scott & Burgan (2005), i.e. grasses (GR fuel models), timber understory (TU fuel models), etc.; and (ii) the model with the highest ROS ranking reflects the fire behaviour expected for that fuel group under the higher flammability conditions and very dry and windy fire-weather conditions.

In FIREBOX WP1, the flammability ranking of land-use classes is derived from a “fire selectivity” analysis, which measures how frequently each land-use class burns relative to its



availability (Figure 1). This selectivity index is then used as a proxy for flammability to generate a ranking that supports an objective and reproducible assignment of fuel models.

However, to adopt this approach, it is necessary to start from land-use classes that exhibit different levels of flammability and can therefore be ordered along a gradient. Moreover, to map fuel models at the national scale using this method, one must rely on a detailed land-use classification harmonised across the entire national territory. Combining these two aspects is not straightforward, as harmonised large-scale land-use classifications do not necessarily incorporate information related to flammability and were not developed with vegetation flammability in mind, but rather other functional aspects (e.g., habitat maps focus on species communities and their structure). For the purposes of the FIREBOX project, we therefore hypothesised that the Forest Type classification available in most Italian regions (e.g., La Mantia et al. 2001, Pignetti et al. 2004, Garfi & Marchetti 2011) could also represent a flammability gradient. Indeed, Forest Types are identified based on several attributes, many of which correlate with flammability, such as the dominant tree species (which can determine different fuel beds), more or less xeric site conditions, soil pH, prevailing elevation, thermophily, and the specific composition of the understory, including the abundance of more or less flammable species (Camerano et al., 2008).

Taking advantage of the opportunity offered by the new Italian Forest Map (CFI) (Mattioli et al. 2025), it was possible to use a nationally harmonised map regarding forest category, i.e., the dominant tree species, while also incorporating all the spatial information available on Forest Types within each region (or other classifications used at regional level).

As for non-forest land-use classes, the only nationally harmonised map currently available is Corine Land Cover (2018 update). However, a Corine class is very broad, spans a wide geographic gradient, and may encompass a wide range of flammability conditions. For this reason, we decided to further segment the CLC-2018 classes by adopting flammability proxies such as the phytoclimatic zone (alpine, temperate, Mediterranean), north–south exposure, and spectral indices such as NDVI, which can discriminate vegetation differences within the same Corine class and represent a proxy of flammability properties.

To test this approach, we calculated the selectivity index for the land-use classes available in the CFI (i.e., Forest Types) for forest vegetation and for those derived from the segmentation



of CLC classes for herbaceous, shrub, and burnable agricultural vegetation. The hypothesis was that land-use classes would not show the same selectivity index values but could instead be ordered along an increasing selectivity gradient.

Once this was verified, we developed an algorithm capable of automatically generating fuel model maps by assigning sets of fuel models to land-use classes based on their flammability ranking. The expected outcome was a fuel model map that accurately reflects the flammability gradient present in a given territory and can therefore be used as input for applications based on the Rothermel (1972) model, e.g. CNR simulator (see Deliverable 3.2), FlamMap (Finney, 2004), to conduct gradient analyses, including Burn Probability maps or rankings into fire hazard classes based on the fireline intensity. These represent the main types of analyses carried out within Regional Fire Management Plans under Law 353/2000, the Italian Framework Law on wildfires, and consequently, the tool we developed may have important applications for wildfire risk analysis at both regional and national park scales.

2. Data architecture and national harmonisation framework

The development of a nationally harmonised fuel model map requires the integration of heterogeneous spatial data that differ in origin, purpose, spatial resolution, and conceptual structure. Unlike local or regional fuel mapping exercises, the objective of WP1 was to construct a single, coherent, wall-to-wall representation of fuel models for the entire Italian territory. This needed a data architecture capable of reconciling differences among land-use classification systems, administrative regions, and ecological zones.

2.1. Terminology and Classification Framework

To create cross-walks between different classification systems, e.g. CFI regional forest types, Corine land cover classes, the following fuel classes were adopted:

- **Fuel group:** a broad vegetation category representing the dominant vegetation type driving fire behaviour (i.e., grasses, shrubs, coniferous forests fuelbeds, broadleaved forests fuelbeds, burnable agriculture) that groups the “fuel macro-classes”.



- **Fuel macro-class (MC):** a classification level within each fuel group, derived from existing land-cover or forest categories (IV level CLCC classes for grasses, shrubs and burnable agriculture; del Favero forest categories for forests from CFI-2020) (Table 1).
- **Fuel sub-class (SC):** a further subdivision of each fuel macro-class, defined either by more detailed regional vegetation typologies (CFI forest types – *TipiLoc*) or, for non-forest vegetation, by the segmentation of macro-classes according to environmental variables such as phytoclimatic zone, aspect, NDVI.

2.2. Italian Forest Map (CFI2020)

The backbone of the forest component of the workflow is the new Italian Forest Map (CFI2020) (Mattioli et al. 2025), which represents the first nationally harmonised cartographic product providing a consistent classification of forest categories across Italy (Table 1). The CFI distinguishes forest categories primarily based on the dominant tree species (e.g., beech forests, oak forests, pine forests, fir forests), ensuring cross-regional comparability.

In addition to forest categories, many regions provide detailed local forest typologies (*TipiLoc*), which describe forest types at finer ecological and spatial resolution. Despite forest types differ from one region to another, they incorporate information related to: (i) dominant and co-dominant species composition; (ii) site moisture regime (xeric vs. mesic conditions); (iii) elevation and thermophily; (iv) soil characteristics; (v) understory composition.

Although the CFI was not originally designed to represent a flammability gradient, many of the ecological attributes used to define forest categories and forest types correlate with fuel structure and fire behaviour potential. For example, pine-dominated forest categories exhibit higher surface-area-to-volume ratios in litter fuels compared to other conifers, while xeric oak forest types tend to be associated to flammable understory vegetation when compared to mesic beech forest types.

However, the level of typological detail varies substantially among regions. Some regions map more than 30 forest types, while others map fewer than 10. To ensure methodological coherence, a threshold of 15 *TipiLoc* classes was adopted as a decision rule for segmentation. Regions exceeding this threshold retained *TipiLoc* as direct fuel sub-classes, whereas regions below this threshold required additional structural segmentation (see Section 3). This choice



was motivated by the need to guarantee sufficient variability for computing meaningful fire selectivity indices without artificially inflating the number of sub-classes in regions already characterized by detailed typological mapping.

Table 1. Forest macro-classes derived from the CFI categories.

Cl_CFI	Macro-class	Tipologia
AB	31201	Abetine
AF	31102	Aceri-frassineti e aceri-tiglieti
AL	31103	Formazioni di altre latifoglie caducifoglie
AM	31204	Abieti-faggeti e abetine miste
AN	31105	Alneti e altre formazioni dei suoli idrici
AQ	31106	Altri querceti caducifogli
AR	31107	Betuleti, corileti e altre formazioni arboree transitorie
CA	31108	Castagneti
CE	31109	Cerrete
CS	31210	Formazioni di altre conifere
EU	31111	Eucalitti
FA	31112	Faggete
FR	31113	Formazioni ripariali
LC	31214	Lariceti, lariceti-cembrete e cembrete
LE	31115	Leccete
LS	31116	Formazioni di altre latifoglie sempreverdi
MT	31217	Pinete di pino montano
MU	31218	Pinete di pino mugo
OS	31220	Orno-Ostrieti
PA	31221	Pinete di pino d'Aleppo
PD	31222	Pinete di pino domestico
PE	31223	Peccete
PF	31224	Piceo-faggeti
PL	31225	Pinete di pino silano, pino loricato e altri pini sporadici
PM	31226	Pinete di pino marittimo
PN	31227	Pinete di pino nero
PS	31228	Pinete di pino silvestre
QC	31129	Querceto-carpineti e carpineti
QF	31130	Querceti di farnia
QR	31131	Querceti di roverella
QV	31132	Querceti di rovere
SU	31133	Sugherete



2.3. Corine Land Cover 2018

Non-forest land uses were represented using the Corine Land Cover (CLC) 2018, fourth level (ISPRA/SINA 2018). CLC is the European land use and land cover mapping project developed within the Copernicus Land Monitoring Service, which adopts a hierarchical legend structured across three levels, up to 44 classes. For Italy, ISPRA produced in 2018 a fourth-level refinement that further details some third-level classes (particularly agricultural and forest areas), providing a more detailed representation of national specificities (Table 2). In this case as well, the vector dataset was rasterized at 100 m and reprojected to EPSG:3035. The CLC_CODE classes were used as the reference key to link with the CFI and as a completion layer in areas not covered by the Forest Map, in order to obtain a continuous land use/land cover map.

Although CLC provides consistent land-use categories across the European Union, its thematic structure is designed primarily for land-use and habitat monitoring rather than fire behaviour analysis. Moreover, CLC classes are often broad and may encompass substantial ecological variability. A single CLC class may span: (i) different climatic zones; (ii) contrasting productivity levels; (iii) distinct fuel continuity patterns.

Therefore, using CLC classes directly as fuel mapping units would not capture internal flammability gradients. To overcome this limitation, additional segmentation criteria were introduced, integrating environmental and structural proxies that modulate fuel characteristics.

Table 2. Decoding of the Corine Land Cover Level IV code

Cod CLC	Corine Land Cover
111	Zone residenziali a tessuto continuo
112	Zone residenziali a tessuto discontinuo e rado
121	Aree industriali, commerciali e dei servizi pubblici e privati
1211	Aree industriali o artigianali
122	Reti stradali, ferroviarie e infrastrutture tecniche
123	Aree portuali
124	Aeroporti
131	Aree estrattive



Cod CLC	Corine Land Cover
132	Discariche
133	Cantieri
141	Aree verdi urbane
142	Aree ricreative e sportive
211	Seminativi in aree non irrigue
2111	Colture intensive
2112	Colture estensive
212	Seminativi in aree irrigue
213	Risaie
221	Vigneti
222	Frutteti e frutti minori
223	Oliveti
231	Prati stabili (foraggiere permanenti)
241	Colture temporanee associate a colture permanenti
242	Sistemi colturali e particellari complessi
243	Aree prevalentemente occupate da colture agrarie con spazi naturali
244	Aree agroforestali
3111	Boschi a prevalenza di querce e altre latifoglie sempreverdi (quali leccio e sughera)
3112	Boschi a prevalenza di querce caducifoglie (cerro e/o roverella e/o farnetto e/o rovere e/o farnia)
3114	Boschi a prevalenza di castagno
3115	Boschi a prevalenza di faggio
3116	Boschi a prevalenza di igrofite (quali salici e/o pioppi e/o ontani, ecc.)
3117	Boschi ed ex-piantagioni a prevalenza di latifoglie esotiche (quali robinia e ailanto)
3121	Boschi a prevalenza di pini mediterranei e cipressi (pino domestico, pino marittimo, pino d'aleppo)
3122	Boschi a prevalenza di pini oro-mediterranei e montani (pino nero e laricio, pino silvestre, pino loricato)
3123	Boschi a prevalenza di abeti (quali bianco e/o rosso)
3131	Boschi misti a prevalenza di latifoglie
3132	Boschi misti a prevalenza di conifere
3211	Praterie continue
3212	Praterie discontinue
323	Aree a vegetazione sclerofilla



Cod CLC	Corine Land Cover
3231	Macchia alta
3232	Macchia bassa e garighe
324	Aree a vegetazione boschiva ed arbustiva in evoluzione
3241	Aree a ricolonizzazione naturale
331	Spiagge, dune e sabbie
332	Rocce nude, falesie, rupi, affioramenti
333	Aree con vegetazione rada
334	Aree percorse da incendi
411	Paludi interne
512	Bacini d'acqua
521	Lagune

2.3.1. Phytoclimatic zonation

Italy spans three major phytoclimatic domains that differ substantially in temperature regimes, drought intensity, vegetation composition and fire traits: (i) Alpine; (ii) Temperate; (iii) Mediterranean. Consequently, the same CLC code, e.g. 3211 – Continuous grasslands (Table 2), experiences prolonged summer drought and recurrent fires in the Mediterranean area, whereas Alpine grasslands are subject to shorter fire seasons and lower fire frequencies. Consequently, even within the same CLC class, flammability may differ markedly between climatic zones. For this reason, phytoclimatic zonation was incorporated into the segmentation of non-forest fuel classes and into the definition of fuel type categories (see Deliverable 1.2). This ensures that identical structural classes located in different climatic contexts are not assumed to exhibit equivalent flammability and fire behaviour potential.

To segment non-forest classes into phytoclimatic zones, a global map of Koppen-Geiger classes at 1 km resolution was used (Beck et al., 2023), available at: <https://www.gloh2o.org/koppen/>. The global Koppen-Geiger data were extracted for Italy and then grouped into three categories: (i) Alpine; (ii) Temperate; (iii) Mediterranean following Table 3. The data were then re-sampled to 20 m resolution and the boundaries of Italian communes and transformed to EPSG:3035.



Table 3. Aggregating Koppen-Geiger classes into major phytoclimatic zones.

Phytoclimatic zone	Koppen/Geiger class
Alpine	‘Cold, dry summer, warm summer’; ‘Cold, no dry season, warm summer’; ‘Cold, no dry season, cold summer’; ‘Polar, tundra’.
Temperate	‘Temperate, no dry season, hot summer’; ‘Temperate, no dry season, warm summer’.
Mediterranean	‘Arid, steppe, cold’; ‘Temperate, dry summer, hot summer’; ‘Temperate, dry summer, warm summer’.

2.3.2. Terrain aspect

Topographic exposure is a key control on microclimatic conditions, vegetation characteristics and fuel moisture dynamics. South-facing slopes in the Northern Hemisphere receive higher solar radiation, typically resulting in: (i) lower fuel moisture content; (ii) increased evapotranspiration; (iii) faster drying rates. Conversely, north-facing slopes tend to retain higher moisture and support denser vegetation in certain contexts. Aspect was therefore dichotomised into north ($\leq 90^\circ, \geq 270^\circ$) versus south ($91-269^\circ$) exposure classes and incorporated into sub-class segmentation. This simple but robust distinction introduces a microclimatic dimension into fuel differentiation without introducing excessive complexity at national scale.

The topographic component was considered using a Digital Elevation Model at 20 m resolution for Italy. The DEM raster dataset is available at <http://www.pcn.minambiente.it/viewer/>. From the DEM, the aspect variable was derived in degrees using the built-in aspect function in QGIS version 3.32. Flat areas were manually assigned a value of 180° (i.e. southern aspect). The layer was subsequently transformed to EPSG:3035.

2.3.3. Canopy cover

Canopy cover in forests controls the amount of light reaching the understory and consequently the potential for plants functional groups such as grasses and shrubs that might display flammability traits depending on the phytoclimatic zone, site conditions and the forest type. Stand canopy openness was characterized using Tree Cover Density (TCD) derived from the Copernicus Land Monitoring Service (High Resolution Layer – Tree Cover Density 2018–2021). The product, also available at a spatial resolution of 100 m consistent with the other



information layers used, expresses the percentage of tree cover (0–100%) (Figure 5). The dataset was reprojected to EPSG:3035 to ensure consistency with the other layers.

2.3.4. NDVI as structural proxy

Normalized Difference Vegetation Index (NDVI) provides a spectral proxy for vegetation greenness and productivity. While NDVI does not directly measure fuel load or structure, it correlates with: (i) biomass accumulation; (ii) canopy density; (iii) vegetation vigour (Carlson and Ripley, 1997).

NDVI is a widely used spectral index for quantifying vegetation presence and condition. It is calculated as the normalized ratio between near-infrared (NIR) reflectance—typically high for healthy vegetation—and red (RED) reflectance, which is strongly absorbed by chlorophyll.

$$\text{NDVI} = (\text{NIR} - \text{RED}) / (\text{NIR} + \text{RED})$$

NDVI values range from -1 to $+1$. Values close to zero or negative indicate non-vegetated surfaces (water, bare soil, rocks), while medium to high values (0.3 – 0.8) are associated with active and healthy vegetation. In this study, NDVI was calculated from Sentinel-2 imagery acquired during the summer period of 2021–2025 (May–September). Images were filtered using a cloud cover threshold of 70%, and calculations were done using Google Earth Engine. The original 10 m resolution data were resampled to 100 m and reprojected to EPSG:3035.

NDVI distributions were analysed within each macro-class of non-forest vegetation, and the 75th percentile was selected as a threshold to distinguish relatively denser subsets from more open formations. The choice of the 75th percentile was motivated by the need to identify structurally distinct subsets while minimizing sensitivity to extreme values and noise. By combining NDVI-based segmentation with aspect and phytoclimatic zone, it was possible to introduce structural differentiation within otherwise broad CLC classes.

2.3.5. Fire perimeter dataset

The empirical foundation of the flammability ranking lies in the harmonised wildfire perimeter dataset developed in WP2 (see Deliverable 2.1). This dataset includes individual fire polygons for the period 2007–2024, corrected for topological errors and standardised in a common coordinate reference system. For each region, wildfire perimeters were rasterized and



intersected with fuel sub-classes to compute annual burned area proportions. The temporal depth (17+ years) ensures that selectivity estimates are not driven by single extreme fire seasons but reflect recurring patterns.

It is important to emphasise that fire occurrence is influenced by multiple factors, including ignition patterns and suppression efficiency. Nevertheless, when aggregated over a sufficiently long time period and large spatial extent, fire selectivity provides a robust proxy for relative flammability differences among land-use classes.

3. Algorithm workflow

The workflow is built on a two-scale data architecture (Figure 1). At the regional scale, the workflow first involves land-cover segmentation, the definition of fuel sub-classes, then the computation of fire selectivity for each fuel sub-class, in order to capture local ecological specificities as accurately as possible. At the national scale, regional selectivity tables are aggregated, all sub-classes within a macro-class are ranked, and the set of fuel models attributed to each macro-class is associated to a sub-class based on the clustering of the selectivity index. This separation between regional and national levels allows the method to preserve regional ecological and fire governance variability while still achieving national standardisation in fuel model assignment.

3.1. Regional Workflow: Sub-Class Segmentation and Raster Construction

The regional workflow represents the first operational stage of the methodology and constitutes the core spatial processing phase. All operations described in this section were implemented in R, primarily using the `terra`, `sf`, `dplyr`, and `fasterize` libraries. Processing was conducted region by region, following standard Italian administrative boundaries, to preserve ecological heterogeneity, and to apply local forest type classifications while ensuring national harmonisation at later stages.

The objective of this phase is to produce, for each region: (i) a raster map of fuel sub-classes covering the entire territory; (ii) a regional database linking sub-classes to macro-classes and fuel groups; (iii) the necessary spatial units for computing fire selectivity indices.



To delineate the study area, the administrative boundaries of Italian regions were used, extracted in order according to the regional code (Cod_reg) from the national ISTAT 2025 shapefile (Table 2). The dataset, originally in the WGS84 CRS, was transformed to EPSG:3035 and used to clip all raster layers to the administrative boundaries, ensuring that all processing remained confined within the regional borders.

The segmentation procedure at the regional level follows a structured sequence:

1. Load and harmonise spatial datasets;
2. Clip all layers to the regional boundary;
3. Construct forest sub-classes from CFI;
4. Construct non-forest sub-classes from CLC;
5. Integrate structural proxies (aspect, NDVI, phytoclimatic region);
6. Merge forest and non-forest layers into a unified sub-class raster.

Each region was processed independently.

Table 2. Regions of Italy and the regional code used in the algorithm

Regione	Cod_reg	Regione	Cod_reg
Piemonte	01	Abruzzo	13
VdA	02	Molise	14
Lombardia	03	Campania	15
Veneto	05	Puglia	16
FVG	06	Basilicata	17
Liguria	07	Calabria	18
Emilia-Romagna	08	Sicilia	19
Toscana	09	Sardegna	20
Umbria	10	Bolzano	21
Marche	11	Trento	22
Lazio	12		



3.1.1. Forest sub-class construction

As described, regions differ in the number of mapped forest types (TipiLoc). To manage this variability, a threshold of 15 TipiLoc per region was adopted. Two cases were defined:

- **Case A: Regions with more than 15 TipiLoc**

If the number of distinct TipiLoc within a region exceeds 15 the fuel sub-classes coincide with the TipiLoc:

$$\text{Fuel Sub-Class} = \text{TipiLoc}$$

In this case, the typological detail is considered sufficient to capture ecological variability relevant to flammability. Each TipiLoc becomes a direct fuel sub-class.

- **Case B: Regions with 15 or fewer TipiLoc**

If the number of TipiLoc is ≤ 15 , further structural differentiation is introduced. Each forest macro-class is subdivided according to: (i) Terrain aspect (North vs South); (ii) Canopy cover (greater or lower than 60%).

Thus:

$$\text{Fuel Sub-Class} = \text{Macro-Class} \times \text{Aspect} \times \text{Canopy Class}$$

This rule increases the number of sub-classes in regions with limited typological details, ensuring that fire selectivity analysis is not constrained by overly coarse classification. The 60% canopy cover threshold was selected as a structural break between relatively open stands and denser formations, consistent with fuel continuity and shading effects on surface fuel moisture.

3.1.2. Non-forest sub-class construction

For non-forest vegetation (grasslands, shrublands, transitional formations, agricultural areas), CLC classes were further segmented to introduce structural differentiation.

- **Aspect segmentation**

All burnable CLC macro-classes were first subdivided by aspect:

(i) north-facing cells ($\leq 90^\circ, \geq 270^\circ$); (ii) south-facing cells ($91-269^\circ$).

This introduces a microclimatic dimension into flammability differentiation.



- **NDVI-based segmentation**

Within each macro-class, NDVI values were extracted and the 75th percentile was computed. Cells were classified as: (i) High NDVI (\geq 75th percentile); (ii) Low NDVI ($<$ 75th percentile).

The rationale for using the 75th percentile rather than the median is to isolate relatively denser subsets while avoiding excessive fragmentation.

- **Phytoclimatic segmentation**

For all non-forest burnable classes, phytoclimatic zonation was incorporated:

$$\text{Sub-Class} = \text{Macro-Class} \times \text{Aspect} \times \text{NDVI} \times \text{Phytoclimate}$$

This ensures that identical structural classes in Alpine and Mediterranean contexts are treated as distinct sub-classes.

3.1.3. Agricultural areas sub-class construction

Agricultural burnable classes were subdivided exclusively by phytoclimatic zone:

$$\text{Sub-Class} = \text{Agriculture} \times \text{Phytoclimate}$$

NDVI segmentation was not applied to agriculture to avoid confounding crop phenology with structural fuel characteristics.

3.1.4. Coding strategy and compositional logic

To maintain traceability of segmentation levels, sub-class codes were constructed using composite numeric encoding. Each code embeds hierarchical information:

- Macro-class identifier;
- Structural segmentation (aspect, NDVI, canopy);
- Phytoclimatic zone.

This compositional logic allows back-tracing from any sub-class to its parent macro-class and fuel group. Non-burnable classes (urban, bare ground, water bodies) were retained as constant codes and excluded from selectivity analysis.



3.1.5. Raster integration and mosaic logic

After forest and non-forest sub-class rasters were constructed separately, they were merged using priority rules:

1. Forest raster has precedence where CFI data are available;
2. Non-forest raster fills remaining areas;
3. Non-burnable classes are retained unchanged.

The `terra::cover()` and `terra::mosaic()` functions were used to integrate rasters while preserving hierarchical precedence.

The result is a wall-to-wall raster at 20 m resolution of fuel sub-classes for each region, projected in EPSG:3035 to ensure national spatial consistency.

3.1.6. Output of regional segmentation phase

For each region, the workflow produces: (i) a raster file: `region_code_subclass.tif`; (ii) a table linking: sub-class code; macro-class; fuel group; structural segmentation attributes.

These outputs constitute the input layer for fire selectivity computation (Section 6).

3.1.7. Methodological considerations

The segmentation procedure balances two competing needs:

1. Sufficient granularity to detect flammability gradients;
2. Avoidance of excessive fragmentation leading to unstable selectivity estimates.

By combining typological detail (where available) with structural proxies (where necessary), the workflow achieves a consistent national framework while respecting regional ecological and fire governance diversity (e.g., fire prevention and fire suppression organization). The segmentation phase is thus not merely a technical preprocessing step, but a conceptual translation of vegetation classification into potential flammability units suitable for ranking flammability.



3.2. Fire Selectivity Computation and Statistical Aggregation

The fire selectivity analysis constitutes the empirical core of the FIREBOX calibration framework. This phase transforms the spatial intersection between wildfire perimeters and fuel sub-classes into a quantitative flammability gradient, which is subsequently used for fuel model assignment at national scale. The computation is conducted at regional level and subsequently aggregated to produce a harmonised national database.

3.2.1. Conceptual definition of fire selectivity

Fire selectivity measures how frequently a given fuel macro-class (index level 1) and sub-class (index level 2) burns relative to its spatial availability. In ecological terms, it represents a selection ratio: if a class burns proportionally more than its area share, it is considered positively selected by fire. Conversely, if it burns less than expected given its area, it is considered negatively selected.

In the context of this deliverable, selectivity is interpreted as a proxy for relative flammability under historical fire-weather conditions. It is important to emphasise that selectivity does not measure intrinsic fuel combustibility in isolation, but rather the combined effect of fuel structure, spatial continuity, moisture regime, landscape configuration, fire spread dynamics. When averaged over long time series and large spatial domains, selectivity provides a robust ranking variable suitable for calibrating the flammability gradient between and within macro-classes.

3.2.2. Macro-class selectivity index (Level 1)

For each region r , fuel macro-class i , and year t , the annual burned proportion is defined as:

$$p_{m,r,t} = \frac{B_{m,r,t}}{A_{m,r}}$$

where:

- $B_{m,r,t}$ = burned area of macro-class i in region r during year t ;
- $A_{m,r}$ = total available flammable area of macro-class i in region r .

Burned area is computed by rasterizing wildfire perimeters for each year (see Deliverable 2.1) and intersecting them with the sub-class raster.



Available area is derived from the frequency of pixels belonging to each macro-class:

$$A_{m,r} = N_{m,r} \times \text{pixel area}$$

where $N_{m,r}$ is the number of pixels of macro-class i . This formulation ensures consistency between numerator and denominator, as both are derived from the same raster grid (EPSG:3035).

The multi-annual selectivity index for macro-class i in region r is computed as:

$$S_{m,r}^{(1)} = \frac{1}{T} \sum_{t=1}^T \frac{B_{m,r,t}}{A_{m,r}}$$

where:

- $B_{m,r,t}$ = total burned area within macro-class m ;
- $A_{m,r}$ = total area of macro-class m .

This Level 1 index captures the general fire propensity of broader vegetation categories (e.g., pine conifer forests vs. beech broadleaved forests vs. shrublands).

3.2.3. Sub-class selectivity index (Level 2)

For each region r , fuel sub-class i , and year t , the annual burned proportion is defined as:

$$p_{i,r,t} = \frac{B_{i,r,t}}{A_{i,r}}$$

where:

- $B_{i,r,t}$ = burned area of sub-class i in region r during year t ;
- $A_{i,r}$ = total available flammable area of sub-class i in region r .

Burned area is computed by rasterizing wildfire perimeters for each year (see Deliverable 2.1) and intersecting them with the sub-class raster.

Available area is derived from the frequency of pixels belonging to each sub-class:

$$A_{i,r} = N_{i,r} \times \text{pixel area}$$



where $N_{i,r}$ is the number of pixels of sub-class i . This formulation ensures consistency between numerator and denominator, as both are derived from the same raster grid (EPSG:3035).

The multi-annual selectivity index for sub-class i in region r is computed as:

$$S_{i,r}^{(2)} = \frac{1}{T} \sum_{t=1}^T p_{i,r,t}$$

where T is the total number of years (2007–2024). Averaging across years reduces sensitivity to extreme fire seasons and interannual variability in ignition patterns. This index captures intra-macro-class variability and represents the fine-scale flammability signal.

3.2.4. Final selectivity index

The final selectivity index assigned to each sub-class combines both levels:

$$S_{i,r}^{final} = S_{m,r}^{(1)} + S_{i,r}^{(2)}$$

This additive formulation ensures that macro-class fire susceptibility influences all sub-classes within it and that sub-class deviations from macro-level average are preserved.

3.2.5. Regional implementation

For each region:

1. Annual wildfire perimeters (2007–2024) are rasterized.
2. Burned pixel counts are extracted per sub-class using `terra::freq()`.
3. Total pixel counts per sub-class are computed.
4. Annual burned proportions are calculated.
5. Multi-annual averages are derived.
6. Macro-class and sub-class indices are merged.
7. The final selectivity index is stored in a regional table.



Each regional table includes:

- Sub-class code;
- Macro-class;
- Fuel group;
- Total area;
- Mean burned proportion;
- Selectivity index Level 1;
- Selectivity index Level 2;
- Final Selectivity index.

3.2.6. National aggregation

All regional tables are concatenated into a single national selectivity database. This aggregation step preserves regional ecological variability and enables national clustering for fuel model assignment (Section 4). At this stage, no clustering or fuel model assignment occurs. The database represents a purely empirical ranking of land-use classes based on observed fire occurrence.

The statistical properties and robustness of the approach are strengthened by several methodological choices: first, the use of a 17-year time window mitigates the influence of anomalous years through temporal averaging; second, area normalisation based on proportional burned area ensures comparability among classes with different spatial extents. Additionally, excluding non-burnable classes (urban, water, and bare ground) from the selectivity computation prevents an artificial dilution of gradients. Finally, very small sub-classes are retained but explicitly flagged for stability checks, reducing the risk of extreme ratios driven by small denominators.

In terms of interpretation limits, it should be emphasised that, although selectivity is used as a flammability proxy, it also reflects historical ignition patterns, suppression efficiency, landscape fragmentation, accessibility, and human influence. Therefore, selectivity should be interpreted as relative fire propensity under the historical fire-regime of a region homogenous



for what concerns fire governance and suppression effort, rather than as intrinsic combustibility under controlled experimental conditions. This distinction is relevant for its practical application: the effectiveness of fuel model assignment based on selectivity may vary depending on the intended use, for example being suitable for hazard mapping but potentially less reliable for detailed fire behaviour simulations.

4. National Fuel Model Association and Clustering

Once regional fire selectivity indices have been computed and merged into a single national database (Section 5), the workflow transitions from empirical analysis to model attribution. This stage consists of associating each fuel sub-class with a specific fire behaviour fuel model from the Scott & Burgan (2005) catalogue.

The objective is not merely to assign fuel models, but to ensure that the resulting national fuel model map:

- Preserves the empirically derived flammability gradient;
- Reflects increasing fire behaviour potential (e.g., rate of spread - ROS);
- Remains consistent across administrative and ecological boundaries.

4.1. Fuel group classification

Before clustering, all macro-classes and sub-classes are harmonised into broader fuel groups, which represent dominant fuel structures and fire behaviour characteristics. The following fuel groups were defined: Forest broadleaves; Forest conifers; Grasses; Shrubs; Grass–shrub formations; Agriculture (burnable); Non-burnable, e.g. urban, bare ground, water (Table 3).

This grouping serves two purposes: (i) it ensures that clustering is performed within ecologically coherent domains; (ii) it prevents artificial mixing of structurally incompatible fuelbeds (e.g., grasslands with closed conifer forests).

Each fuel group is treated independently in the clustering phase.



4.2. Selection of candidate fuel models

For each fuel group, a predefined set of Scott & Burgan (2005) fuel models was selected (Table 4) including some custom fuel models (i.e., 100-114-115-120-140). These models were chosen according to two criteria:

1. Ecological relevance to the macro fuel group (e.g., timber litter models for forests, grass models for herbaceous systems);
2. Coverage of a gradient of rate of spread (ROS) values.

For example:

- Broadleaf forests were associated with models such as TL2, TL4, TL6, etc.;
- Conifer forests were associated with both timber litter and timber-understory models;
- Grasses were associated with GR-type models (e.g., GR1–GR9).

Within each fuel group, candidate fuel models were ordered according to increasing simulated ROS under standardized weather and fuel moisture conditions.

This ordering ensures that: $FM_1 < FM_2 < FM_3 < \dots < FM_k$

where FM_k corresponds to the highest fire behaviour potential within that group.

Table 3. Fuel macro-classes within each fuel group.

Fuel group	CFI / CLCC macro_classes*
Forest broadleaves	31102, 31103, 31105, 31106, 31107, 31108, 31109, 31111, 31112, 31113, 31115, 31116, 31129, 31130, 31131, 31132, 31133, 31220
Forest conifer	31201, 31204, 31210, 31214, 31217, 31221, 31222, 31223, 31224, 31225, 31226, 31227, 31228
Grasses	241, 242, 243, 244, 3211, 3212, 321
Shrubs	3231, 3232, 3241, 90 (converted from 31218 in CFI), 91 (converted from 31119 in CFI)
Grass–shrub	322, 333, 334
Agriculture (burnable)	212, 213, 221, 222, 231, 223, 211, 2111, 2112
Non-burnable - urban	111, 112, 121, 122, 123, 124, 131, 132, 133, 141, 142, 1211
Non-burnable – bare ground	331, 332, 335
Non-burnable – water	411, 412, 421, 422, 423, 511, 512, 521, 523

*Macro-class codes refers to Table 1 and Table 2.



Table 4. Standard fuel models (Scott & Burgan 2005) and custom models assigned to fuel group and ordered by increasing rate of spread.

Fuel group	Fuel model codes
Grasses	100, 114, 115 , 101, 102, 103, 105, 104, 106
Grass-shrub	120 , 121, 122, 123, 124
Shrubs alp, temp	140 , 141, 143, 142
Shrub med	142, 146, 153 , 147, 154 , 149
Forest broadleaves	182, 184, 186, 189, 161, 162
Forest conifers	183, 185, 187, 188, 165, 164, 163
Agriculture (burnable)	93, 100 , 114, 115, 140, 101
Urban (not burnable)	91
Bare ground (not burnable)	99
Water (not burnable)	98

*fuel models in bold are custom

4.3. Clustering procedure

The final selectivity index S_i^{final} represents a continuous flammability gradient across sub-classes. However, standard fuel models consist of discrete categories. Therefore, the continuous empirical gradient must be partitioned into k discrete groups, where k equals the number of candidate fuel models within the fuel group.

Rather than using arbitrary thresholds (e.g., equal quantiles), a **K-means clustering** algorithm was applied for the following reasons: (i) it minimizes within-group variance of selectivity; (ii) it maximizes separation among clusters; (iii) it produces data-driven partitions rather than arbitrary splits; (iv) it adapts to skewed or non-normal distributions.

Thus, clustering ensures that fuel model assignment reflects statistically coherent selectivity classes rather than fixed percentiles.

For each fuel group the clustering extracts all sub-classes belonging to the group, standardize the selectivity index, apply K-means clustering with:

$$k = \text{number of candidate fuel models in the group}$$

The algorithm partitions sub-classes into k clusters by minimizing the sum of squared distances within clusters, where C_1, C_2, \dots, C_k represent clusters ordered by increasing mean selectivity.



After the clustering, the algorithm computes the mean selectivity value for each cluster, rank clusters from lowest to highest mean selectivity and associate clusters deterministically to fuel models ranked by increasing ROS.

Thus:

$$\begin{aligned} C_1 &\rightarrow FM_1 \\ C_2 &\rightarrow FM_2 \\ &\vdots \\ C_k &\rightarrow FM_k \end{aligned}$$

This monotonic association guarantees coherence between empirical fire propensity (selectivity index) and simulated potential fire behaviour (ROS). In other words, sub-classes that burn more frequently in historical records are assigned fuel models that produce higher simulated ROS under comparable conditions.

It is important to note that clustering is performed at national scale, not regionally. This design choice ensures that fuel model assignment is consistent across regional boundaries, identical vegetation types in different regions are evaluated within the same statistical framework and that the national fuel model map is coherent and not fragmented by regional artefacts.

4.4. Production of the fuel model map

Once cluster-to-model mapping is defined:

1. A lookup table is generated:
 - Sub-class \rightarrow Cluster ID \rightarrow Fuel Model Code.
2. The regional sub-class raster is reclassified according to this table.
3. Regional fuel model rasters are mosaicked to produce a national wall-to-wall fuel model map.

The resulting Fuel Model raster (Annex A):

- Is coded with Scott & Burgan and custom fuel model IDs;
- Is projected in EPSG:3035;
- Is directly compatible with Rothermel-based simulators.



4.5. Implications

The use of clustering ensures that the discretization of flammability into fuel models is grounded in statistical structure rather than arbitrary class breaks. Indeed, the clustering-based approach differs fundamentally from physiognomic matching (Table 5). The clustering approach relies on a set of key assumptions: it presumes that the selectivity distribution contains meaningful information on flammability, that the candidate fuel models adequately span a representative rate-of-spread (ROS) gradient, and that the resulting clusters are internally homogeneous in terms of fire propensity.

At the same time, several methodological boundaries should be acknowledged, including potential sensitivity to skewed distributions, dependence on the number and composition of the candidate fuel models considered, and the unavoidable discretisation of what is a continuous gradient. Despite these limitations, the proposed method still represents a substantial step forward compared with purely physiognomic fuel model mapping at the national scale.

Table 5. Differences between the FIREBOX approach and physiognomic matching

Traditional Approach	FIRE-BOX Approach
Static vegetation–model pairing	Empirically ranked pairing
Expert-driven	Data-driven
Often local	Nationally harmonised
No statistical partitioning	K-means clustering



5. Validation and Performance Assessment

The methodological framework developed in WP1 is based on an empirically derived flammability gradient and a clustering-based discretization into fuel models. Given the novelty of this approach at national scale, a validation phase was conducted to assess:

- The sub-class segmentation reflects a gradient in fire selectivity which is coherent with expected fire behaviour gradients displayed by Italian vegetation classes;
- The potential fireline intensity simulated at regional scale is coherent with analyses currently calibrated at regional scale by Regional Fire Management plans. The test was carried out in Piemonte and Lombardia;
- The potential fireline intensity simulated with the national fuel model map displays higher values within historical fire perimeters than outside fire perimeters.

5.1. Coherence in the selectivity index gradient of macro- and sub-classes

The gradients in fire selectivity of sub-classes both across fuel types and macro-classes within fuel types were coherent with expected fire behaviour gradients displayed by Italian vegetation classes. Within the forest fuel types, the macro-classes with the highest fire selectivity were Aleppo pine forests and cork oak forests which are dominant in fire-prone Mediterranean areas (Figure 2). In contrast, the macro-classes with the lowest selectivity values were silver fir and mixed silver fir and beech forests, which are typical of cooler climate mountainous areas. For non-forest fuel types, shrub and grass-shrub formations had the highest selectivity indices, followed by grasses and burnable agriculture. Within macro-classes, fire selectivity gradients largely followed phytoclimatic gradients with sub-classes occurring in southern regions and Mediterranean climates consistently selected by fire at greater rates than subclasses in northern and alpine regions. This coherency was observed across forest (Figure 3) and non-forest (Figure 4) fuel types.

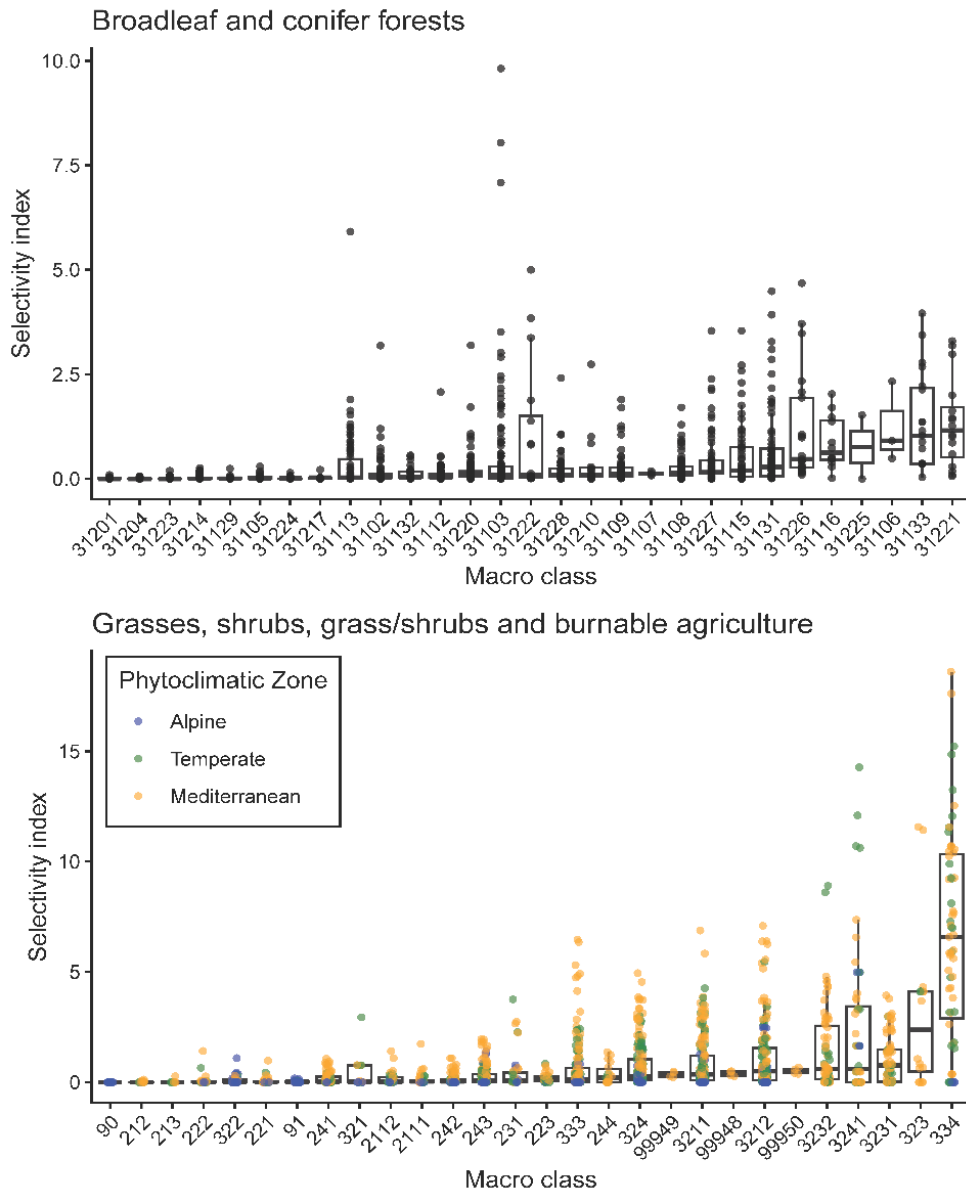


Figure 2. Gradients in fire selectivity index across forest macro-classes (top panel) and non-forest macro-classes (bottom panel). Boxplots show the variation (median, upper and lower quartiles) within each macro-class. Points are the selectivity index values for sub-classes within each macro-class.

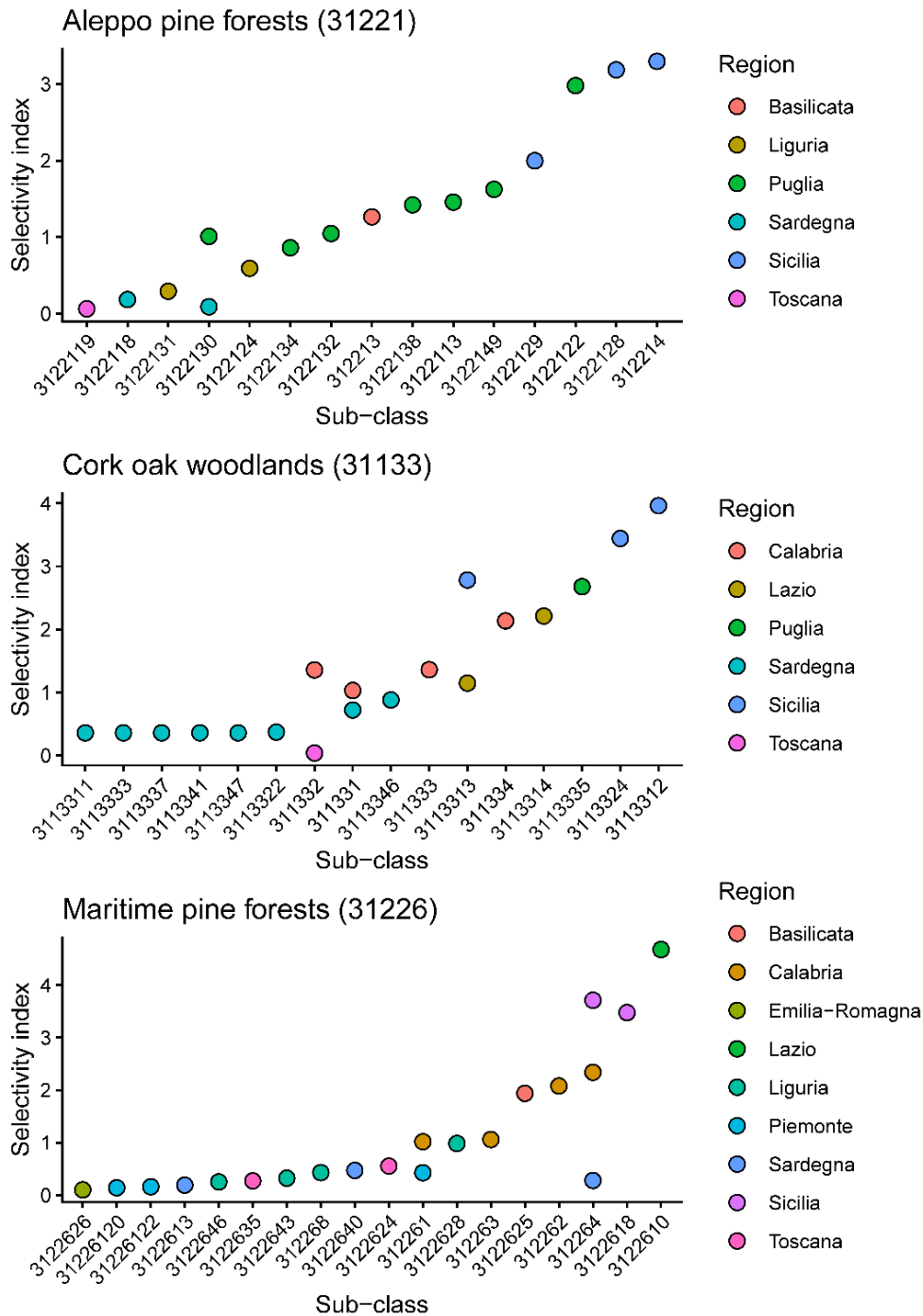


Figure 3. Gradients in fire selectivity index across three forest macro-classes. Points are values for sub-classes within each macro-class. Colours represent regions of Italy.

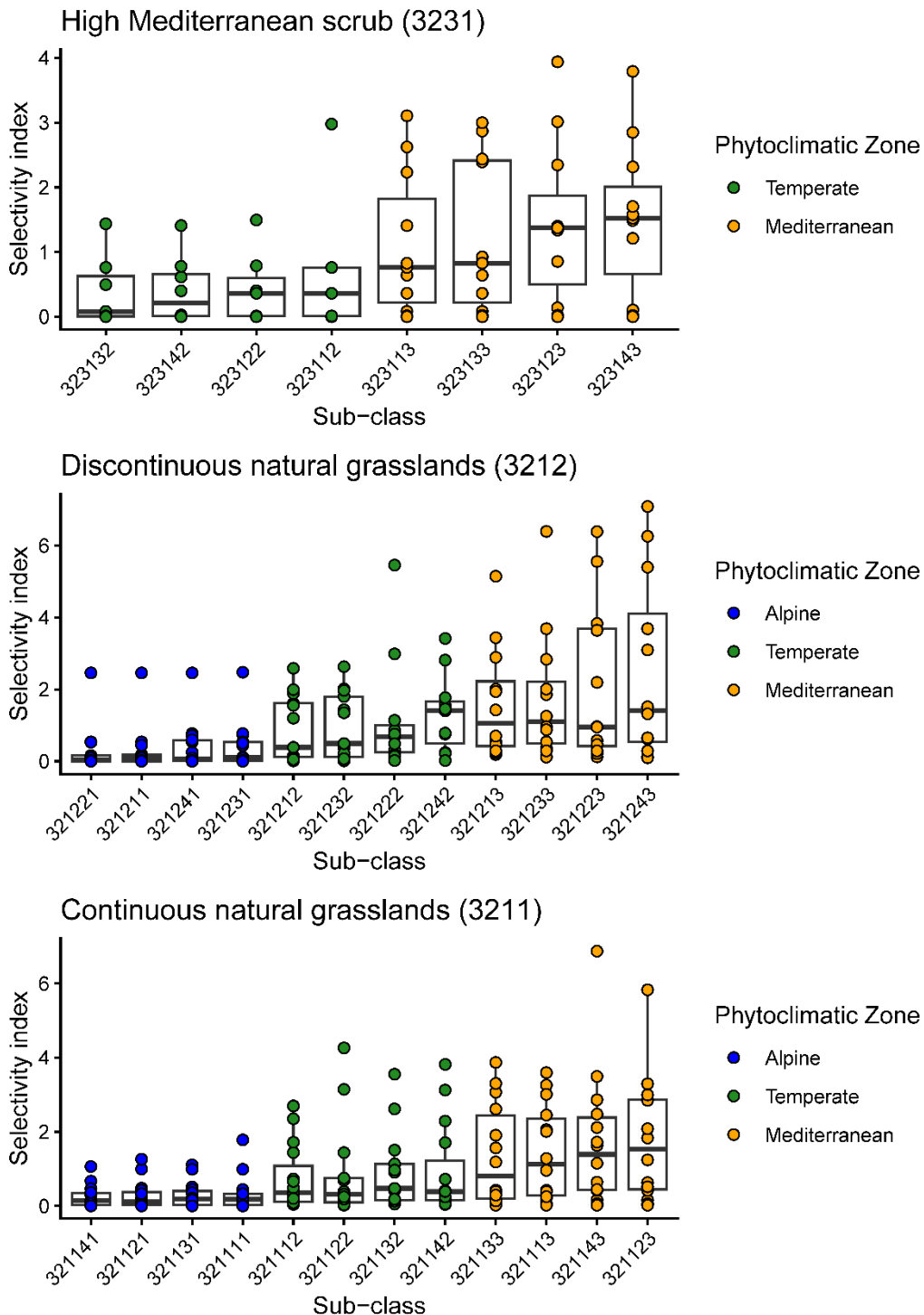


Figure 4. Gradients in fire selectivity index across three non-forest macro-classes. Points are values for sub-classes within each macro-class. Boxplots show the variation (median, upper and lower quartiles) within each sub-class. Colours represent phytoclimatic zones.



5.2. Regional-scale simulated potential fireline intensity

The validation process of the fuel model map consisted, first, of merging all regional maps into a single national map. Subsequently, potential fire behaviour was simulated using FlamMap, version 6.2, developed by the USDA Forest Service (Finney, 2004). This software enables the simulation, mapping, and analysis of potential wildfire behaviour characteristics in a two-dimensional environment by implementing the semi-empirical fire spread model developed by Rothermel (1972).

The application of this model requires input parameters describing :

- topography, described by elevation (m a.s.l.), slope (°), and aspect (°N) maps;
- canopy cover (%);
- fuel characteristics, represented by the fuel model map (Scott & Burgan, 2005), which is the subject of the present validation analysis.

Meteorological inputs were also provided, including fuel moisture content and wind characteristics. Fuel moisture conditions were defined according to the standard D2L1 moisture scenario described by Scott and Burgan (2005). Wind conditions were represented by a topography-driven wind scenario, with wind direction aligned with the maximum slope and a constant wind speed of 20 km h⁻¹.

Based on these input data and parameters, the fireline intensity (FI) output was obtained through FlamMap simulations. This output was subsequently used in the validation analyses described in the following paragraphs.

5.3. Assessment of potential fireline intensity relative to historical fire perimeters

To evaluate the simulation outputs, a historical validation analysis was performed by comparing the simulated fireline intensity (kW m⁻¹) values inside and outside the perimeters of historical wildfires. The validation was conducted both at the national scale and at the phytoclimatic zone level, distinguishing among Alpine, Temperate, and Mediterranean zones. Historical wildfire perimeters were derived from the National Fire Database for the 2007–2024 period (see Deliverable 2.1). Based on this spatial dataset, 10,000 random points were generated inside and 10,000 random points outside the burned perimeters across the national



territory, considering only burnable land covers. Similarly, for the phytoclimatic-level analysis, 5,000 random points were distributed inside and 5,000 outside the burned areas within each phytoclimatic zone.

Simulated Fireline Intensity values were then extracted from the raster pixels corresponding to each randomly generated point.

The random point generation procedure, both inside and outside the fire perimeters, and the extraction of the corresponding fireline intensity values were repeated ten times.

5.3.1. Comparison of mean fireline intensity values

For each iteration, the mean and standard deviation of fireline intensity were calculated separately for points located inside and outside the historical fire perimeters (Table 6).

Table 6 – Mean value and standard deviation of *Fireline Intensity* (FI), calculated for each iteration separately for the groups of points located inside and outside the historical wildfire perimeters.

Iteration	Group	National		Alpine zone		Temperate zone		Mediterranean zone	
		FI mean (kW/m)	FI St.Dev. (kW/m)	FI mean (kW/m)	FI St.Dev. (kW/m)	FI mean (kW/m)	FI St.Dev. (kW/m)	FI mean (kW/m)	FI St.Dev. (kW/m)
1	outside	84.10	338.95	45.26	149.31	26.99	164.51	142.08	483.86
2	outside	91.75	380.23	45.23	126.04	29.03	166.04	149.96	526.70
3	outside	94.36	380.85	44.68	129.16	33.48	210.35	149.36	521.03
4	outside	96.63	411.11	43.75	109.01	32.84	194.56	157.71	565.42
5	outside	90.87	368.45	44.05	156.47	30.58	182.27	143.69	509.13
6	outside	95.44	388.67	46.58	166.25	30.07	182.84	134.88	467.38
7	outside	95.44	396.36	41.56	82.19	30.71	193.38	133.29	460.93
8	outside	95.40	402.01	41.87	95.86	30.95	184.61	140.60	502.11
9	outside	107.15	444.79	43.34	124.48	28.97	161.75	151.14	530.93
10	outside	92.96	387.93	43.56	121.36	29.74	164.72	140.99	495.78
1	inside	639.30	1353.26	107.02	252.39	146.34	512.12	708.87	1380.25
2	inside	632.96	1317.75	97.13	226.99	156.02	541.01	696.05	1410.70
3	inside	648.60	1371.30	108.12	254.73	158.91	545.13	697.85	1416.73
4	inside	677.87	1396.21	105.38	238.49	162.14	576.16	678.75	1374.34
5	inside	623.72	1297.23	100.97	236.31	156.44	534.49	694.46	1426.34
6	inside	616.03	1291.97	98.64	232.36	170.35	593.82	691.02	1381.90
7	inside	641.88	1345.32	108.64	252.09	160.32	549.52	719.54	1435.34
8	inside	630.06	1339.80	108.80	264.90	151.14	511.82	708.83	1446.74
9	inside	661.11	1383.46	102.83	237.12	172.63	583.69	706.91	1422.06
10	inside	647.41	1361.95	101.55	235.63	163.54	579.47	719.74	1420.91



5.3.2. Statistical test

Subsequently, t-tests were performed for each validation analysis using the mean value obtained from each iteration in order to assess the statistical significance of the differences in simulated fireline intensity between the groups of points located inside and outside the historical wildfire perimeters.

The mean intensity was consistently higher for points located within burned areas compared to those located outside, both at the national scale and at the phytoclimatic zone level (Table 7). This difference was found to be statistically significant, as illustrated in Figures 5 and 6.

Table 7 – Results of the t-tests comparing simulated *Fireline Intensity* (FI) values between points located inside and outside historical wildfire perimeters, reported for each validation analysis at the national and phytoclimatic zone levels.

Validation zone	Inside points		Outside points		t	p
	FI mean (kW/m)	FI S.E.	FI mean (kW/m)	FI S.E.		
National	641.89	5.74	94.41	1.82	90.92	<0.001
Alpine	103.91	1.36	43.99	0.49	41.64	<0.001
Temperate	159.78	2.53	30.33	0.59	49.71	<0.001
Mediterranean	702.20	4.10	144.37	2.41	117.31	<0.001

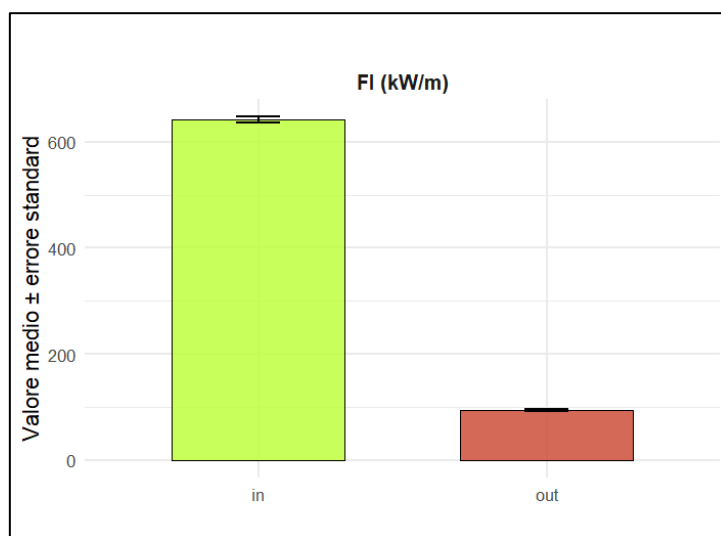


Figure 5. Comparison of mean Fireline Intensity (FI) values across the ten iterations for points located inside (in) and outside (out) historical wildfire perimeters at the national scale, including standard error.

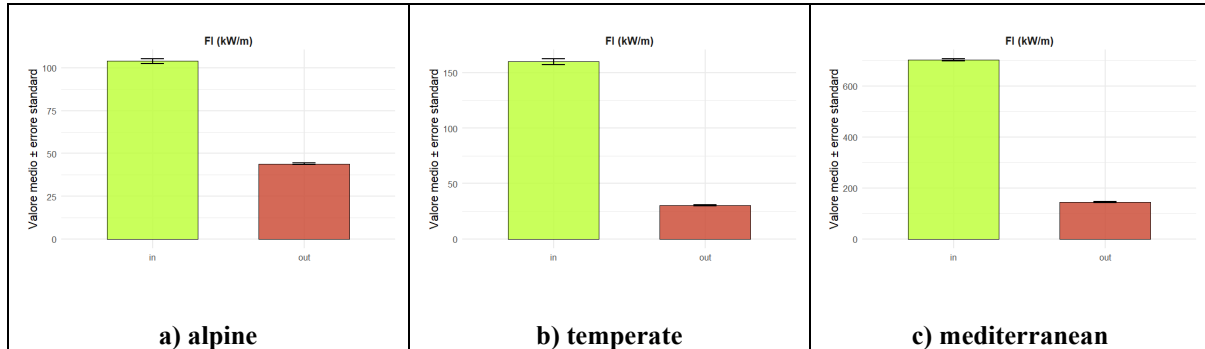


Figure 6. Comparison of mean Fireline Intensity (FI) values across the ten iterations for points located inside (in) and outside (out) historical wildfire perimeters, for each phytoclimatic zone, including standard error.

5.3.3. Graphical comparison of fireline intensity values

The distribution of simulated fireline intensity values was visually analyzed for the groups of points located inside and outside historical wildfire perimeters, with boxplots and density distributions plots.

Boxplots were generated to compare the distribution of FI values between the two groups at both the national scale and across phytoclimatic zones (Figure 7 and 8). FI values associated with points located inside historical wildfire perimeters exhibited higher median values and a distribution shifted towards greater intensity levels compared to those located outside burned areas.

Density distribution plots confirmed these results at national scale level (Figure 9) and at phytoclimatic zone level (Figure 10), highlighting the higher frequency of elevated FI values, whereas lower values of FI were more frequent in points outside burned areas.

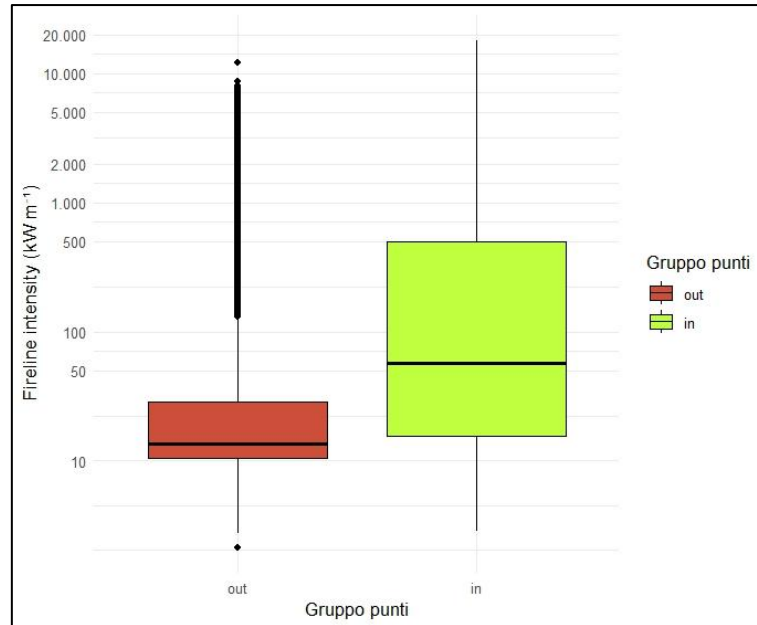


Figure 7. Comparison of fireline intensity (FI) values for all randomly distributed points located inside (in) and outside (out) historical wildfire perimeters at the national scale (y-axis values are displayed on a logarithmic scale).

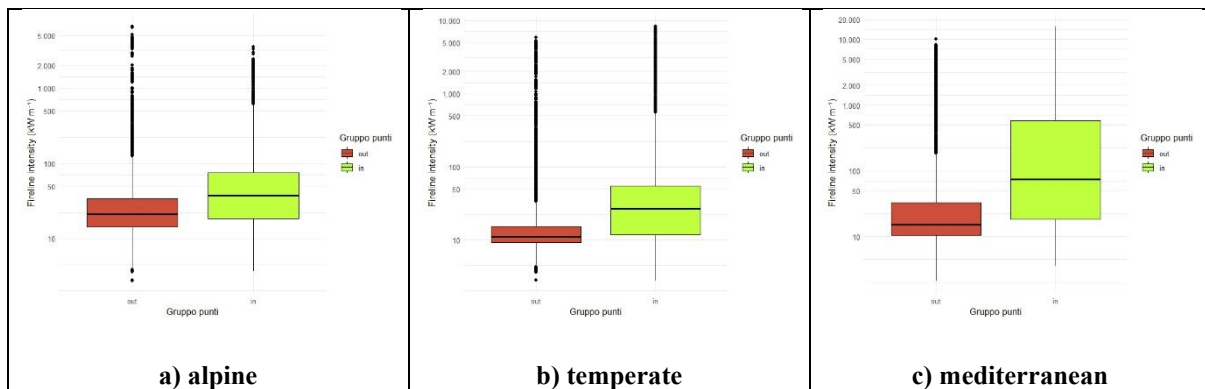


Figure 8. Comparison of fireline intensity (FI) values for all randomly distributed points located inside (in) and outside (out) historical wildfire perimeters at the phytoclimatic zone scale (y-axis values are displayed on a logarithmic scale).

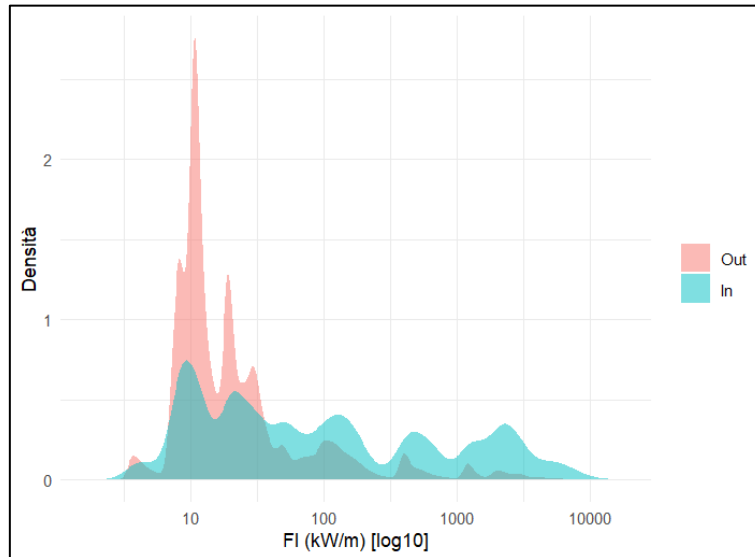


Figure 9. Comparison of the frequency distributions of fireline intensity (FI) values for points located inside (in) and outside (out) historical wildfire perimeters at the national scale (x-axis values are displayed on a logarithmic scale).

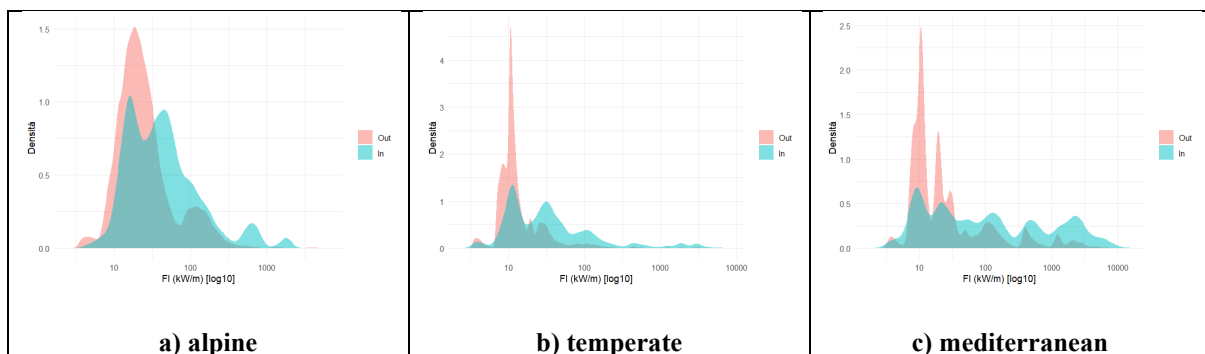


Figure 10. Comparison of the frequency distributions of fireline intensity (FI) values for points located inside (in) and outside (out) historical wildfire perimeters at the national scale (x-axis values are displayed on a logarithmic scale).



6. Fuel model map methodological assumptions and limitations

The methodological framework developed in WP1 is grounded in empirical fire selectivity and statistical clustering. While this approach represents a significant advancement over purely physiognomic fuel model assignment, it is important to explicitly state the assumptions and limitations underlying the methodology.

The methodology is grounded in the central assumption that historical fire occurrence can serve as a proxy for relative flammability among land-use classes. The selectivity index measures how frequently a class burns relative to its spatial availability. However, observed fire occurrence within a large area such as Italian administrative Regions is shaped not only by intrinsic fuel properties but also by broader socio-ecological drivers. These include ignition density, probability of weather extremes (e.g. exposure to strong winds), suppression efficiency and accessibility, landscape configuration, proximity to infrastructures and settlements, and management practices. Consequently, selectivity reflects realised fire behaviour under historical conditions rather than intrinsic combustibility measured in experimental settings. The extended temporal window (2007–2024) and the averaging of yearly selectivity ratios reduce sensitivity to short-term anomalies, yet structural shifts in ignition patterns or fire management strategies may still influence selectivity gradients over time.

A closely related limitation concerns suppression and ignition biases. Fire perimeters represent events that were able to spread prior to containment. Although suppression effectiveness can be considered constant within an administrative Region, suppression effectiveness varies across regions, particularly after 2017 because of the suppression of the State Forestry Corp (Kirshner et al. 2026), and as a consequence of road density (i.e. accessibility), and interaction with fuel flammability. Remote fuel complexes may accumulate larger burned areas due to delayed intervention. Similarly, human-caused ignitions are spatially clustered, particularly near agricultural and peri-urban areas, potentially inflating burned proportions independently of structural fuel characteristics. Fuels that sustain low intensity fires under mild weather (e.g., fuelbeds in beech forests) may be rapidly contained in most years, reducing their burned proportion despite they might potentially express high intensity under rare weather extremes (Maringer et al. 2016, Moris et al. 2018). The framework we created not explicitly model ignition probability or suppression intensity; rather, it assumes that, when averaged across long



temporal and broad spatial scales, these factors do not irreversibly distort the relative ranking among broad vegetation categories. Future refinements could integrate ignition density weighting to disentangle exposure from structural flammability (Spadoni et al. 2023).

Structural differentiation within broad land-cover classes is partly achieved through NDVI segmentation. While multi-year composites and percentile thresholds reduce sensitivity to phenological noise, NDVI remains an indirect proxy: it captures greenness rather than fuel load, is influenced by interannual variability, and does not distinguish live from dead biomass. Likewise, the national raster resolution (aligned to EPSG:3035 grids) imposes constraints on the detection of fine-scale heterogeneity, small sub-classes, and narrow landscape features. The adopted resolution represents a compromise between computational feasibility and ecological representation at national scale, acknowledging that local applications may require finer inputs. Another methodological constraint arises from the discretisation of a continuous selectivity gradient. Selectivity values are inherently continuous, but clustering (K-means) converts them into discrete fuel model classes for compatibility with standard fuel model catalogues (Anderson 1982, Scott & Burgan 2005) and operational simulators. Although clustering minimises within-class variance, it inevitably introduces boundary effects: sub-classes near cluster thresholds may be sensitive to small variations in selectivity or parameter settings. Discretisation is therefore a practical necessity, but it simplifies underlying gradients.

Finally, the calibration reflects historical fire regimes over 2007–2024. Climate change may alter fire season length, extreme fire-weather frequency, drought intensity, and vegetation structure, potentially shifting selectivity gradients in the future. A key strength of the framework, however, is its adaptability: the selectivity computation and clustering steps can be rerun with updated fire perimeter datasets, enabling periodic recalibration of the fuel model map.

In summary, the methodology assumes that historical selectivity adequately captures relative flammability, that ignition and suppression biases do not irreversibly distort ranking, that NDVI and terrain factors sufficiently approximate structural variability within broad classes, and that clustering provides a stable operational discretisation. Within these assumptions, the framework offers a transparent, reproducible, and nationally harmonised alternative to purely physiognomic or expert-based fuel model assignments, supporting robust and reproducible fire behaviour modelling.



7. Fuel Type map

While the fuel model map is designed to parameterize fire behaviour simulations under the Rothermel (1972) framework, WP1 also produced a complementary product: the national Fuel Type Map (Annex B). Unlike fuel models, which are directly linked to numerical parameter sets used in fire spread simulations, fuel types provide an interpretable categorisation of vegetation units according to flammability classes and ecological context. The fuel type map therefore represents a simplified and communicative representation of the flammability gradient emerging from the selectivity analysis.

It is important to distinguish clearly between the two products produced within WP1. The Fuel Model Map represents a spatial layer of discrete parameter sets used to simulate fire behaviour metrics such as rate of spread (ROS), fireline intensity (FI), and flame length within models based on the Rothermel equations. The Fuel Type Map, by contrast, represents a categorisation of vegetation units into flammability classes within ecological groups and is not directly tied to a specific set of model parameters. Fuel types therefore act as an intermediate interpretative layer between land-cover information and fuel model assignment, providing a simplified representation of flammability gradients derived from fire selectivity.

The Fuel Type Map serves three main purposes. First, it supports communication with land managers and non-technical stakeholders who require a clear interpretation of vegetation flammability without relying on technical fuel model codes. Second, it provides a transparent flammability ranking derived from empirical fire occurrence data and independent of specific fuel model catalogues. Third, it facilitates integration into regional fire management plans and planning instruments required under Italian Law 353/2000.

The conceptual structure of the Fuel Type Map is also consistent with the hierarchical fuel classification developed in Deliverable D1.1. In that deliverable, surface fuels were organised into a national classification composed of three hierarchical levels: Fuel group, MacroFuelType, and FuelType. Fuel groups represent broad vegetation formations controlling the dominant fuel structure driving fire behaviour, including grasses, shrubs, broadleaved forests, conifer forests, and burnable agricultural systems. These groups are subdivided into macro fuel types based on ecological and structural attributes such as dominant species composition, litter characteristics, and phytoclimatic context. Individual fuel types then



represent flammability variants within each macro fuel type, reflecting differences in fuel load, vegetation structure, or environmental conditions. The Fuel Type Map produced in WP1 translates this conceptual classification into spatial units derived from land-cover data and the segmentation procedures described in the previous sections.

The mapping of these Fuel type classes builds directly upon the fire selectivity index introduced in Section 5. This index quantifies how frequently each vegetation unit burns relative to its spatial availability, providing an empirical proxy for relative flammability under historical fire regimes. By ranking vegetation classes according to this index, it becomes possible to derive simplified flammability classes that preserve the main gradients observed in fire occurrence while remaining operationally interpretable.

7.1. National flammability thresholds

To define flammability classes in a statistically coherent manner, all regional selectivity indices were pooled into a single national distribution. The resulting distribution was then used to define thresholds for different vegetation groups. Thresholds were computed separately for forest fuels and for non-forest vegetation systems, reflecting their different ecological dynamics and fire regimes.

7.1.1. Forest fuels (broadleaves and conifers separately)

For forest fuel groups, broadleaved and conifer forests were analysed separately to avoid conflating structurally distinct fuelbeds. Three flammability levels were defined using quantiles of the national selectivity distribution. The thresholds correspond to the 33rd and 66th percentiles of the selectivity index (S_i) distribution.

Sub-classes were assigned to flammability levels according to the following rules:

- Low flammability when the S_i is lower than the first threshold ($S_i < Q0.33$)
- Medium flammability when the S_i falls between the two thresholds ($Q0.33 \leq S_i < Q0.66$)
- High flammability when the selectivity index exceeds the upper threshold ($S_i \geq Q0.66$)

This quantile-based partitioning ensures a balanced representation of the selectivity distribution while maintaining national coherence in the classification of forest vegetation types.



7.1.2. Non-forest fuels

For non-forest fuel groups, including grasses, shrublands, and grass–shrub formations, flammability was defined separately for each phytoclimatic zone rather than using national quantiles. Herbaceous and shrub-dominated vegetation systems are strongly influenced by climatic conditions, particularly the contrast between Alpine, temperate, and Mediterranean fire regimes. Applying a single national threshold would therefore risk masking important climatic differences.

For each phytoclimatic zone z , the mean selectivity value was calculated. Sub-classes within the zone were then classified according to whether their selectivity index was below or above the zonal mean:

- Low flammability when $S_i < \bar{S}_z$
- High flammability when $S_i \geq \bar{S}_z$

A two-level classification scheme was adopted for these vegetation systems in order to avoid excessive fragmentation and to reflect the typically bimodal distribution observed in non-forest selectivity values.

7.1.3. Agricultural fuels

Burnable agricultural areas were classified into three flammability levels per phytoclimatic zone using a similar quantile-based approach. However, agricultural fuels differ from natural vegetation systems because fuel structure and continuity are strongly influenced by management practices, crop phenology, harvesting cycles, and irrigation regimes. For this reason, agricultural flammability classes should be interpreted primarily as indicators of relative fire propensity useful for hazard stratification rather than as stable representations of fuel structure.



7.2. Fuel type coding system

Each fuel type is uniquely identified through a hierarchical coding system derived from the classification defined in Deliverable D1.1. The code structure combines information about the fuel group, the macro-class, and the flammability level assigned to the vegetation unit.

The four-digit code follows a hierarchical logic:

Fuel Group identifier + Macro-Class identifier + Flammability rank

This encoding system ensures traceability to the original land-use or vegetation class, guarantees compatibility across regional classifications, and allows future extensions or refinements without altering the logical structure of the classification.

Relationship between fuel types and fuel models

Although fuel types and fuel models are derived from the same selectivity ranking, they serve different operational functions. Fuel models discretize the selectivity gradient into k classes determined by the candidate fuel models associated with each fuel group and are used directly in fire behaviour simulations. Fuel types instead discretize the same gradient into two or three flammability classes depending on the ecological group.

Fuel type classification therefore does not replace fuel model assignment. Rather, it provides an interpretative and communicative layer that can be used to summarise hazard at regional scale, support management zoning and prioritisation of prevention measures, and communicate differences in vegetation flammability without referring to technical fuel model codes.

Together with the fuel model map, the Fuel Type Map contributes to a coherent national framework for representing vegetation flammability and supporting wildfire risk analysis.

8. Operational implications of the Fuel Model and Fuel Type maps

The national Fuel Model Map developed in WP1 should be understood not as a standalone cartographic deliverable, but as a core operational layer that enables the modelling and decision-support architecture of WP3 (RISK BOX) to function in a spatially explicit, harmonised, and reproducible way across the whole of Italy, with a particular focus on National Parks. Within WP3, the map provides the structural fuel input required by both modelling tools



grounded in the Rothermel (1972) surface fire spread equations and driven by raster-based representations of fuels, topography, and weather (Milestone 8). In WP3, the fuel model raster is combined with slope and aspect from a digital elevation model, wind fields, and fuel moisture content to parameterise fire behaviour in operational scenarios. Since each fuel model corresponds to internally consistent parameter sets (e.g., fuel load, surface–area-to-volume ratio, heat content) compatible with other Rothermel based simulators (e.g., FlamMap, Behave+, Rothermel package in R), it can be used as input of these decision support systems to map potential spread trajectories, estimate fireline intensity, and derive indicators such as flame length and crown fire initiation potential—outputs that are particularly relevant for fire hazard analyses and fire risk assessment. This potential has immediate governance relevance under Italian Law 353/2000, which requires to prepare Fire Management Plans (Piani AIB) at both Regional and National Parks scales including hazard mapping, risk assessment, and prevention planning. Whereas traditional approaches to calibrate fuel model maps often rely on expert judgement, and static vegetation-weighting schemes, the WP1 fuel model map enables a shift toward reproducible, mechanistic, simulation-based hazard ranking that privileges intensity-based metrics rather than historical fire occurrence alone, allowing comparisons between administrative Regions and National Parks. At the scale of National Parks and Piani Forestali di Indirizzo Territoriale (PFIT, D.lgs. 34/2018), the fuel model map supports landscape scale deterministic simulations to identify high-intensity propagation corridors, support fuel treatment planning, and integration with vulnerability and exposure modules (e.g., Wildland Urban Interface, see Deliverable 3.3) to construct composite fire risk maps (see Deliverable 3.4). Another strength of this method is that is easy to apply through the years, as vegetation dynamics determine a shift of forest type in a pixel. Importantly, because the WP1 calibration is ranking-based and designed to represent a statistically coherent flammability gradient, it also enables gradient analyses and consistent hazard interpretation across administrative boundaries. In this sense, WP1 delivers more than an input for modelling: it provides the structural foundation for a modern, data-driven, and nationally harmonised wildfire risk governance framework in Italy, which is currently the scope of several national projects such as the SIM coordinated by the Ministry of the Environment.



References

- Anderson, H.E. (1982). Aids to determining fuel models for estimating fire behaviour. USDA Forest Service GTR INT-122.
- Ascoli, D., Vacchiano, G., Motta, R., & Bovio, G. (2015). Building Rothermel fire behaviour fuel models by genetic algorithm optimisation. *International Journal of Wildland Fire*, 24, 317–328.
- Ascoli, D., Moris, J.V., Sil, A., & Fernandes, P. (2022). Using the Rothermel package in R to test standard and custom fuel models against global fire behavior data. *Environmental Sciences Proceedings*, 17, 86.
- Beck, H.E., McVicar, T.R., Vergopolan, N., Berg, A., Lutsko, N.J., Dufour, A., Zeng, Z., Jiang, X., Van Dijk, A.I. and Miralles, D.G. (2023). High-resolution (1 km) Köppen-Geiger maps for 1901–2099 based on constrained CMIP6 projections. *Scientific Data* 10, 724.
- Camerano P., Gottero F., Terzuolo P.G., Varese P. (2008). *Tipi forestali del Piemonte*. IPLA S.p.A., Regione Piemonte, Blu Edizioni, Torino, pp. 216
- Carlson, T. N. & Ripley, D. A. (1997). On the relation between NDVI, fractional vegetation cover, and leaf area index. *Remote Sensing of Environment*. 62, 241-252.
- Cruz, M.G., & Fernandes, P.M. (2008). Development of fuel models for fire behaviour prediction in maritime pine stands. *International Journal of Wildland Fire*, 17, 194–204.
- Finney, M.A. (2004). FlamMap, fire mapping and analysis system. USDA Forest Service, RMRS.
- Garfi, V., & Marchetti, M. (2011). *Tipi forestali e preforestali della regione Molise*. Edizioni dell’Orso Srl.
- Keane, R.E. (2015). Wildland fuel classification and mapping: frameworks, approaches, and applications for fire management. *Forest Ecology and Management*, 294, 43–56.
- Kirschner, J. A., Kirschner, J., Ascoli, D., Moris, J. V., Boustras, G., & Spadoni, G. L. (2026). Evaluating wildfire policy impacts using synthetic controls: a data-driven assessment in Italy. *International Journal of Wildland Fire*, 35(1), WF25107.
- La Mantia, T., Marchetti, M., Gullota, S., & Pasta, S. (2001). Materiali conoscitivi per una classificazione dei tipi forestali e preforestali della Sicilia. II parte: descrizione delle categorie. *L’Italia forestale e montana*, 56(1), 24-47.



- Maringer, J., Wohlgemuth, T., Hacket-Pain, A., Ascoli, D., Berretti, R., & Conedera, M. (2020). Drivers of persistent post-fire recruitment in European beech forests. *Science of the Total Environment*, 699, 134006.
- Mattioli, W., Romano, R., Botticelli, D., Chirici, G., D'Amico, G., Giuliarelli, D., et al. (2025). La Carta Forestale d'Italia (CFI2020): un ritratto aggiornato dei boschi italiani. *Forest@*, 22, 39–44.
- Parresol, B. R., Scott, J. H., Andreu, A., Prichard, S., & Kurth, L. (2012). Developing custom fire behavior fuel models from ecologically complex fuel structures for upper Atlantic Coastal Plain forests. *Forest Ecology and Management*, 273, 50-57.
- Pignatti, G., Terzuolo, P. G., Varese, P., Semerari, P., & Lombardi, V. N. (2004). Criteri per la definizione di tipi forestali nei boschi dell'Appennino meridionale. *Forest@-Journal of Silviculture and Forest Ecology*, 1(2), 112.
- Rothermel, R.C. (1972). A mathematical model for predicting fire spread in wildland fuels. USDA Forest Service Research Paper INT-115.
- Scott, J.H., & Burgan, R.E. (2005). Standard fire behaviour fuel models. USDA Forest Service GTR RMRS-GTR-153.
- Spadoni, G. L., Moris, J. V., Vacchiano, G., Elia, M., Garbarino, M., Sibona, E., ... & Ascoli, D. (2023). Active governance of agro-pastoral, forest and protected areas mitigates wildfire impacts in Italy. *Science of the total environment*, 890, 164281.
- Vacchiano, G., & Ascoli, D. (2015). An implementation of the Rothermel fire spread model in the R programming language. *Fire Technology*, 51(3), 523-535.
- Wu, Z. W., He, H. S., Chang, Y., Liu, Z. H., & Chen, H. W. (2011). Development of customized fire behavior fuel models for boreal forests of northeastern China. *Environmental management*, 48(6), 1148-1157.

ANNEX

Annex A – Fuel Model Map

Annex B – Fuel Type Map